Journal of Solid State Chemistry **155,** 332–341 (2000)
doi:10.1006/jssc.2000.8922, available online at http://www.idealibrary.com on IDEAL®

Investigating the Effects of Guest–Host Interactions on the Properties of Anion-Exchanged Mg–Al Hydrotalcites

François Malherbe[1] and Jean-Pierre Besse

Laboratoire des Matériaux Inorganiques, Université Blaise Pascal, 24 avenue des Landais, 63177 Aubière, France

Received May 8, 2000; in revised form July 19, 2000; accepted August 9, 2000; published online November 29, 2000

A starting [Mg–Al–Cl] LDH, prepared by coprecipitation, was further anion-exchanged to incorporate a variety of anions in the interlayer domain: $(Fe(CN)_6)^{3-}$, $(P_2O_7)^{4-}$, $(V_2O_7)^{4-}$, $(CrO_4)^{2-}$, and $(Cr_2O_7)^{2-}$. The resulting materials were fully characterized using classical techniques like XRPD, FTIR, TGA/DTA, and BET, and their structural modifications studied as a function of calcination temperatures. Under mild calcination, only the oxo-anions were shown to interact strongly with the host matrix. This resulted in a systematic shrinkage of the interlamellar domain, with a negative impact on the surface properties. However, intercalation of oxo-anions proved to be beneficial to thermal stability, the lamellar structure being maintained up to 400°C in the case of the dichromate intercalated [Mg–Al]. A thorough analysis of the FTIR spectra, revealing an evolution in the symmetry of some oxo-anions, confirmed the occurrence of a grafting process. Furthermore, the permanent character of the pillars was evidenced through unsuccessful rehydration and back-exchange reactions.

Key Words: **hydrotalcite; anion exchange; oxo-anions; thermal behavior; layered double hydroxides.**

INTRODUCTION

Layered double hydroxides (LDHs) represent a class of ionic lamellar solids with positively charged layers and exchangeable hydrated gallery anions. They are composed of octahedrally coordinated bivalent (e.g., Mg^{2+}, Ni^{2+}, Zn^{2+}, Cu^{2+}) and trivalent (e.g., Al^{3+}, Cr^{3+}) cations, sharing edges to form infinite brucite-like sheets. Hydrotalcites are generally described by the empirical formula $[M^{2+}_{(1-x)}M^{3+}_x(OH)_2][A^{m-}_{x/m}\cdot nH_2O]$, abbreviated hereafter as $[M^{2+}$–M^{3+}–$A]$, where x may vary from 0.17 to 0.33 (1–3). A represents the m-valent anion necessary to compensate the net positive charge. Their development is of increasing interest due to their potential use in various applications like monitoring environmental wastes, implementing new catalytic systems, or elaborating efficient molecular sieves (4). In the search for pillared layered solids (PLS) that mimic the zeolite-type structure, but possessing larger and more modifiable pores and active sites, LDHs have attracted much attention due to their high anion-exchange capacities (5). A review of such hydrotalcites, intercalated mainly with robust polyoxometalates, has been carried out recently (6), giving a very good insight into this specific property of LDHs as well their potential exploitation as pillared solids. The anion-exchange properties are also of particular importance in the development of heterogeneous catalysts: it sometimes represents the only alternative to incorporate a desired element in the composition of the solid or to increase the loading of a particular metal. When the intercalated LDHs are used as precursors for catalysts, the mixed oxides obtained following high temperature calcination will constitute an intimate and homogeneous mixture of the metallic components giving the material its particular catalytic properties (7). Anion-exchange reactions, along with the high flexibility in the composition of the brucite-like layers, are often considered to be crucial parameters in the tailoring of specific catalytic systems.

We report in this work the preparation and characterization of a series of intercalated magnesium–aluminum hydrotalcites. The various anions used differ in their charge density, geometry, and size, to measure the influence of these parameters on the properties of the final materials. Our main interest was to evaluate the thermal stability of the anion-exchanged LDHs and to monitor their structural evolution as a function of temperature. Here, we present a systematic and comparative study of these different materials over a wide range of temperature. The catalytic activity of the materials has been assessed in the oxidative dehydrogenation of ethylbenzene (8) and in the ethoxylation of butanol (9).

EXPERIMENTAL

Materials

For all preparative procedures, metal chlorides and nitrates, sodium carbonate, sodium hydroxide, sodium

[1]To whom correspondence should be addressed at School of Engineering and Science, Swinburne University of Technology, John Street, Hawthorn, VIC 3122, Australia. Fax: + 61 (0) 3 9214 5267. E-mail: mmalherbe@swin.edu.au.

0022-4596/00 $35.00

metavanadate, potassium dichromate, potassium chromate, potassium hexacyanoferrate(III), and sodium pyrophosphate (all from Fluka) were of analytical grade.

The materials presented in this study have been prepared following existing procedures available in the literature, either for magnesium–aluminum or for other systems: [Mg–Al–Cl], according to Miyata (10); [Mg–Al–$Fe(CN)_6$], following a procedure detailed by Cavalcanti *et al.* (11); [Mg–Al–V_2O_7], according to Twu and Dutta (12); [Mg–Al–CrO_4], referring to Miyata and Okida (13); and [Mg–Al–P_2O_7], as described by Malherbe *et al.* (8).

[Mg–Al–Cr_2O_7] was adapted from the procedure described by de Roy *et al.* (14). A sample of 1.00 g of [Mg–Al–Cl] was soaked in 25 cm^3 of distilled, deionized water and the precipitate was stirred for 1 h under inert nitrogen atmosphere. The pH of the mixture was then adjusted to 6.0 ± 0.1 by dropwise addition of a 2 M solution of HCl. The mixture was kept under magnetic stirring for 1 more h. Then 50 cm^3 of a 0.5 M solution of $K_2Cr_2O_7$ was added, followed by an adjustment of the pH, and the exchanged reaction was left for 2 h. It should be noted that a higher concentration of the incoming anion was used, the main reasons being: (1) to avoid competition with the excess chloride ions added; and (2) the dichromate solution was enough acidic to maintain the mixture at a pH of ~ 6. The final slurry was then washed and centrifuged (3 cycles) and a bright yellow solid was isolated after appropriate drying.

Methods

All materials were examined by powder X-ray powder diffraction (XRPD) with a Siemens D501 diffractometer using Cu$K\alpha$ radiation. The samples, as unoriented powders, were scanned from 2° to 76° (2θ) in steps of 0.08° with a count time of 4 s at each point. The FTIR spectra were recorded on a Perkin–Elmer 2000 FT spectrometer at a resolution of 2 cm^{-1} and averaging 10 scans in the 400- to 4000-cm^{-1} region using the KBr pellet technique. A typical pellet contains ca. 1 wt% sample in KBr. Chemical analyses were performed by inductively coupled plasma (ICP) emission spectroscopy at the Analysis Centre of the CNRS, Vernaison. Thermogravimetric analyses (TGA) were performed on a SETARAM TGA92 thermogravimetric analyzer. Prior to the TGA, all materials were dried at 40°C overnight. The samples were heated between 25 and 1050°C under continuous air flow at a heating rate of 5°C min^{-1} for all data collection. The nitrogen adsorption–desorption isotherms were recorded at liquid nitrogen temperature on a Fison SP1920 instrument. The materials were pretreated as follows: heating in air at 100°C for 16 h followed by degassing for 4 h at 80°C. Pore size distributions were calculated using the Barrett–Joyner–Halenda (BJH) model (15) on the desorption branch.

RESULTS AND DISCUSSION

XRPD of the Fresh Samples

As shown in Fig. 1, all the Mg–Al samples prepared both by coprecipitation and anion exchange displayed the typical X-ray powder diffraction patterns of the hydrotalcite structure. When compared to the parent magnesium–aluminum chloride, all the other materials exhibit a significant expansion of the interlayer domain, which is a good indication of successful anion exchange. Tables 1 and 2 summarize the results of the chemical analyses performed on the hydrotalcites as well as the crystallographic parameters. The amount of water molecules is calculated from the percentage loss as available from the thermogravimetric curves. The elemental composition of the various samples indicates that the Mg/Al ratio in the host matrix is very close to that of the parent material. One general observation that can be

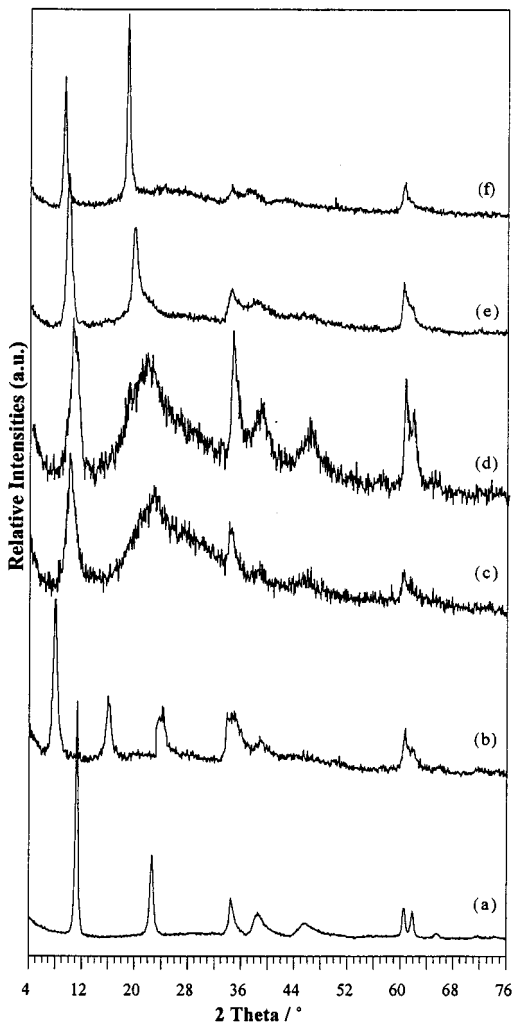

FIG. 1. XRPD patterns of (a) [Mg–Al–Cl], (b) [Mg–Al–$Fe(CN)_6$]. (c) [Mg–Al–P_2O_7], (d) [Mg–Al–V_2O_7], (e) [Mg–Al–CrO_4], and (f) [Mg–Al–Cr_2O_7] hydrotalcites.

TABLE 1
Elemental Chemical Analysis Results and Idealized Formulas of the Synthetic LDHs

Sample	Chemical composition (% wt/wt)	Formula
[Mg–Al–Cl]	Mg(21.09), Al(7.90), Cl(10.03), C(0.12)	$[Mg_{5.98}Al_{2.02}(OH)_{16}]Cl_{1.95}$, $(CO_3)_{0.07}\cdot 7.6H_2O$
[Mg–Al–Fe(CN)$_6$]	Mg(23.21), Al(8.79), Fe(5.55), N(8.35), C(6.8), Cl(0.09)	$[Mg_{5.96}Al_{2.04}(OH)_{16}]$ $(Fe(CN)_6)_{0.62}$, $Cl_{0.02}(CO_3)_{0.07}\cdot 3.4H_2O$
[Mg–Al–P_2O_7]	Mg(22.20), Al(8.47), P(4.58), Cl(0.11), C(0.11)	$[Mg_{5.95}Al_{2.05}(OH)_{16}]$ $(P_2O_7)_{0.48}$, $Cl_{0.02}(CO_3)_{0.06}\cdot 5.1H_2O$
[Mg–Al–V_2O_7]	Mg(22.31), Al(8.45), V(7.32), Cl(0.19), C(0.14)	$[Mg_{5.96}Al_{2.04}(OH)_{16}]$ $(V_2O_7)_{0.47}$, $Cl_{0.03}(CO_3)_{0.08}\cdot 4H_2O$
[Mg–Al–CrO_4]	Mg(21.97), Al(8.41), Cr(7.40), Cl(0.13), C(0.08)	$[Mg_{5.95}Al_{2.05}(OH)_{16}]$ $(CrO_4)_{0.94}$, $Cl_{0.02}(CO_3)_{0\cdot.05}\cdot 4.1H_2O$
[Mg–Al–Cr_2O_7]	Mg(19.43), Al(7.60), Cr(12.94), Cl(0.31)	$[Mg_{5.92}Al_{2.08}(OH)_{16}]$ $(Cr_2O_7)_{0.92}$, $Cl_{0.07}\cdot 3.7H_2O$

made is that all hydrotalcites present a small contamination with carbonate ions, except for the dichromate-exchanged LDH. This is related to the low pH maintained throughout the exchange reaction to stablize the dichromate species. As expected, it also results in a partial dissolution of the brucite-like sheets, the magnesium–aluminum ratio being slightly less, as compared to the other LDHs. With the exception of the pyrovanadate and dichromate anions, the pH of the reaction mixtures was not controlled due to the high basicity of the LDH slurry (ca. 9). For the other species we are not constrained to carry out the exchange reactions within a narrow pH range with respect to issues regarding anion stability (16). However, this is not the case for the pyrovanadate intercalated LDH, for which the pH was constantly maintained at 11 ± 0.1 (12), or for the $(Cr_2O_7)^{2-}$ species, which only exist at pH values lower than 6.

It is interesting to note the difference in crystallinity between the different samples resulting from the anion-exchange reaction. Compared to the parent chloride precursor, which exhibits fine and intense peaks characteristic of a well-crystallized material, the exchanged LDHs tend to give relatively broader peaks. However, a noteworthy difference is observed with the ferricyanide intercalated LDH, which presents a significantly higher crystallinity than the other anion-exchanged hydrotalcites.

Some authors have assigned the poor crystalline state of anion-exchanged LDHs to a disturbance in the stacking sequence of the layers caused essentially by anions adsorbed on the surface (13). The alleged default being less pronounced in [Mg–Al–Fe(CN)$_6$] would thus suggest that the tendency for this anion to be adsorbed is much lower, thence giving an indication of its reactivity with the hydroxylated layers.

Furthermore, these results seem to indicate that the turbostratic effect arising from anion intercalation is not solely dependent on the size of the incoming guest. For example, if the XRPD patterns of the chromate and ferricyanide LDHs are compared, the latter is shown to be more crystalline while it is also the more voluminous of the two. As for these two LDHs, the pH and the concentration of the anion were strictly the same; any influence of the experimental conditions is ruled out. When considering the $(X_2O_7)^{q-}$ anions, which are approximately of the same size and feature close geometry, a significant difference is observed in the crystallinity of the dichromate ($q = 2$) as compared to the pyrovanadate and pyrophosphate ($q = 4$). However, for these anions the pH values of the reaction mixtures are very different and might play a significant role in determining the crystalline state of the final material. The LDHs resulting form intercalation of the tetravalent anions $(P_2O_7)^{4-}$ and $(V_2O_7)^{4-}$; both exhibit an important broadening of the second diffraction peak. A similar behavior has been reported for LDH intercalated with metavanadate (17, 18) and assigned by the authors to a disorder in the periodicity of the (00*l*) planes, possibly related to the formation of polymeric chains in the interlamellar domain. The XRPD

TABLE 2
Composition and Lattice Parameters of [Mg–Al] Layered Double Hydroxides

Parameter	[Mg–Al–Cl]	[Mg–Al–Fe(CN)$_6$]	[Mg–Al–P_2O_7]	[Mg–Al–V_2O_7]	[Mg–Al–CrO_4]	[Mg–Al–Cr_2O_7]
Basal spacing (Å)	7.93	11.25	8.90	8.59	9.03	9.59
Intermetallic distance (*a*; Å)	3.06	3.06	3.06	3.06	3.06	3.06
Mg/Al (molar ratio)	2.96	2.93	2.91	2.93	2.90	2.84
x (degree of substitution)	0.252	0.254	0.256	0.254	0.256	0.260
Anion charge	−1	−3	−4	−4	−2	−2
Anion (moles per unit cell)	1.95	0.62	0.48	0.47	0.94	0.92
$(CO_3)^{2-}$ (moles per unit cells)	0.07	0.07	0.06	0.08	0.05	—
Residual Cl^-	—	0.02	0.02	0.03	0.02	0.07
Effective anion intercalation	—	91	94	93	92	88

patterns of these intercalated LDHs provide clear evidence of the influence of the characteristics of the incoming anion on the structural properties of the resulting material. Steric effect alone cannot account for the observed disturbances and other parameters, such as charge density and reactivity of the anionic species, must be considered.

Thermal Analyses

The thermogravimetric (TG) and differential thermogravimetric (DTG) curves of the materials are shown in Fig. 2. In view of the results shown here, the thermal evolution of hydrotalcite-like materials can be broadly characterized by four main events: evaporation of adsorbed water, elimination of the interlayer structural water, dehydroxylation of the brucite-like sheets, and either loss of the anion (for volatile species like Cl^-, NO_3^-, or CO_{33}^{2-}) or, for nonvolatile species, inclusion of the metallic part in the formation of mixed metal oxides (e.g., CrO_4^{2-}, $Cr_2O_7^{2-}$, $V_2O_7^{2-}$).

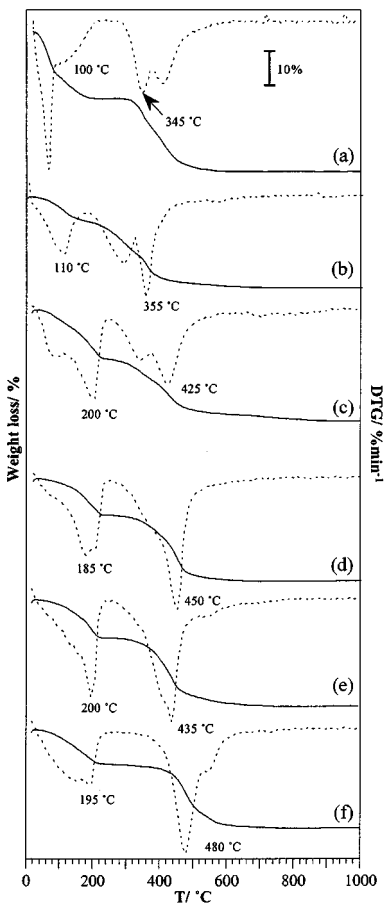

FIG. 2. Thermogravimetric (solid line) and differential thermogravimetric (dashed line) curves of the parent (a) [Mg–Al–Cl] and anion-exchanged LDHs, (b) [Mg–Al–$Fe(CN)_6$], (c) [Mg–Al– P_2O_7], (d) [Mg–Al–V_2O_7], (e) [Mg–Al–CrO_4], and (f) [Mg–Al– Cr_2O_7].

On the other hand, these four steps may or may not be distinct, depending on various factors such as the dryness of the sample, the stability of the intercalated anion, the reactivity of the interlamellar species, or possible guest–host interactions mobilizing the hydroxyl groups. These various possibilities are well-illustrated in the samples presented in this study: the behavior of the each individual sample is shown to be quite distinctive. The parent chloride LDH clearly indicates the presence of a significant amount of adsorbed water molecules that are easily eliminated at temperatures well below 100°C, followed by the loss of interlamellar water up to 200°C. Dehydroxylation of the hydrotalcite framework takes place in the temperature range between 340 and 350°C and finally the chloride anions are lost at temperatures up to 470°C. On comparing the thermogravimetric curves of the different materials, we refer mostly to the temperature at which the DTG curve is at its minimum, i.e., at maximum rate of the weight loss. Given that all the samples have been analyzed under the same conditions, this would represent an adequate basis for the discussion of the different behaviors.

Following anion exchange, two interesting deviations are observed. The first difference concerns the event assigned to the loss of the interlayer water molecules. While in the hexacyanoferrate intercalated LDH this weight loss occurs within approximately the same temperature range as in the chloride precursor, it is shifted at a slightly higher temperature in the other materials. When considering the nature of the anion present in the interlamellar region the opposite trend should normally be observed. By taking into account only steric hindrance considerations, the other anions, much bulkier than the simple halide, should create greater voids between the sheets and facilitate the elimination of water. Although the X-ray powder diffraction patterns of the exchanged materials evidenced a significant expansion of the interlayer (Fig. 1), no such tendency is observed. With regard to the relative charge density of the brucite-like sheets and the electronic repulsion of charged species, the chloride anions being monovalent, the occupancy of the interlayer domain by the monovalent chloride anion would be normally higher than that of the other anions, thus offering less space for the dynamic water molecules to be eliminated. However, from the results presented here, it occurs that the shift observed in the elimination of the water molecules affect mostly the oxo-anion intercalated LDHs. Another peculiar aspect of this first weight loss, as it can be determined from the DTG curves, concerns the rate at which the interlamellar water was lost. Again, the nature of the anion seems to play an important role: for example, in the chloride and hexacyanoferrate LDHs this event occurs over a wide range of temperature, the shape of the differential curve indicating that the process is relatively slow. Conversely, in the other materials two trends are observed: a slow rate at lower temperatures and a faster one when a certain limit

temperature is achieved. Above 180°C all the residual water molecules are eliminated rapidly. These observations suggest that the interlamellar water molecules are held differently in the materials considered, according to the local environment. The more likely explanation would be that they are involved in the solvation of the anions through hydrogen bonding. These hydrogen bonds are expected to be stronger with the oxo-anions than with chloride or the hexacyanoferrate anions. Moreover, the asymmetric shape of the DTG curves observed in the cases of the oxo-anion intercalated LDHs might be an indication of the existence of two types of interlamellar water molecules: free ones and those solvating the anionic species. The existence of different kinds of interlayer water has been reported in [Mg–Al–OH] (20, 21) and [Mg–Al–ClO_4] (3) but these were correlated to the charge density of the hydroxylated sheets. In this work, the comparative thermogravimetric data suggest an influence of the interlayer anions.

The second interesting point to observe concerns the dehydroxylation step, which in the chloride precursor is at its maximum at 345°C. This temperature is in good agreement with the relative stability of brucite and gibbsite, which decompose respectively at 350 and 300°C (22). The process occurs at almost the same temperature (355°C) in the hexacyanoferrate LDH. When compared to the other LDHs studied in this work a singular behavior is observed in [Mg–Al–$Fe(CN)_6$]: with the interlayer anion being less stable than the hydroxylated sheets, a significant weight loss occurs before the dehydroxylation, as the $[Fe(CN)_6]^{3-}$ complex decomposes to expel the (CN) groups. These results are in good agreement with detailed studies of this LDH previously reported in the literature (23–25). On the other hand when the interlayer region is occupied by oxo-anions, the dehydroxylation is shown to take place at much higher temperatures: from 425°C with the pyrophosphate LDH upto 480°C with [Mg–Al–Cr_2O_7]. In the latter compound, the existence of a plateau (220–400°C), a temperature range during which no thermogravimetric event is observed, indicates a relatively stable material. When compared to the parent chloride LDH, for which a similar behavior is observed between 180 and 300°C, it is clear that dehydroxylation of the brucite-like sheets can be delayed on purpose through the incorporation of an appropriate anion. We have recently reported a similar behavior in some nickel–aluminum hydrotalcites (26), suggesting that a substantial amount of the hydroxyl groups of the brucite-like sheets are involved in a network of hydrogen bonding involving the intercalated anions. However, given the extent of the first weight loss associated with the elimination of interlayer water molecules, it is believed that partial dehydroxylation also occurs in this temperature range (up to 200°C according to the nature of the anion). The plausibility of such an event has been envisaged by various authors (27–32) and ascribed to the occurrence of a grafting process of the oxo-anion on the hydroxylated sheets. Not only does this comparative study seem to reinforce this assumption, but with the hexacyanoferrate LDH as a counter example, it appears that the grafting phenomenon would be specific to oxo-anions. It is believed that this specificity is the result of both the stability of oxo-anions and the reactivity of the terminal oxygen atoms that provide the anion with the ability to condense on the hydroxylated sheets.

XRPD of the Thermally Treated LDHs

The structural modifications induced by moderate thermal treatment of the intercalated LDHs was investigated by X-ray powder diffraction and the main results are summarized in Fig. 3. The solids were calcined under normal conditions at the desired temperature for 16 h and analyzed without cooling. A general comment that can be made for all the LDHs considered is that the moderate thermal treatment is systematically accompanied by a broadening of the diffraction peaks and a decrease in their intensity. It is believed that this is most probably related to the loss of interlamellar water molecules causing a loss of cohesion between the LDH plates. The elimination of these structural water molecules, involved in the maintaining of a regular layer stacking, would bring about a partial collapse of the structure: the rigidity of the framework is thus somewhat lost. Also, as suggested by Reichle *et al.* (19), evaporation of the interlayer water is achieved through the brucite-like sheets and will thus cause some disturbances in their arrangement.

The interaction of the guest anion with the hydroxylated sheets is clearly shown to be dependent on the intrinsic characteristics of the anionic species. The maximum temperature for which a lamellar structure, identified by the presence of (00*l*) diffraction lines, can be maintained is shown to be a function of the intercalated anion. The XRPD patterns of the chloride LDH give some indication of the stability of the hydrotalcite structure in the absence of pillaring agents. It is also worthwhile to note that both anion stability and reactivity are important in determining the preservation of the hydrotalcite structure. The hexacyanoferrate anion being decomposed at relatively low temperature, the crystallinity of the material is shown to be significantly affected at temperatures as low as 200°C and a total collapse of the structure occurs at 250°C. On the other hand, the pyrophosphate anion proved to be particularly reactive and, compared to the other oxo-anions, a notable difference is that the lamellar structure is lost at much lower temperatures. This seems to corroborate the DTG data illustrated in Fig. 3, where the weight loss ascribed to dehydroxylation is doubled: with one minimum peaking at 335°C and the other at 425°C. It is suspected that this is related to partial dehydroxylation following interaction of the anion with the hydroxylated layer resulting in the collapse of the LDH

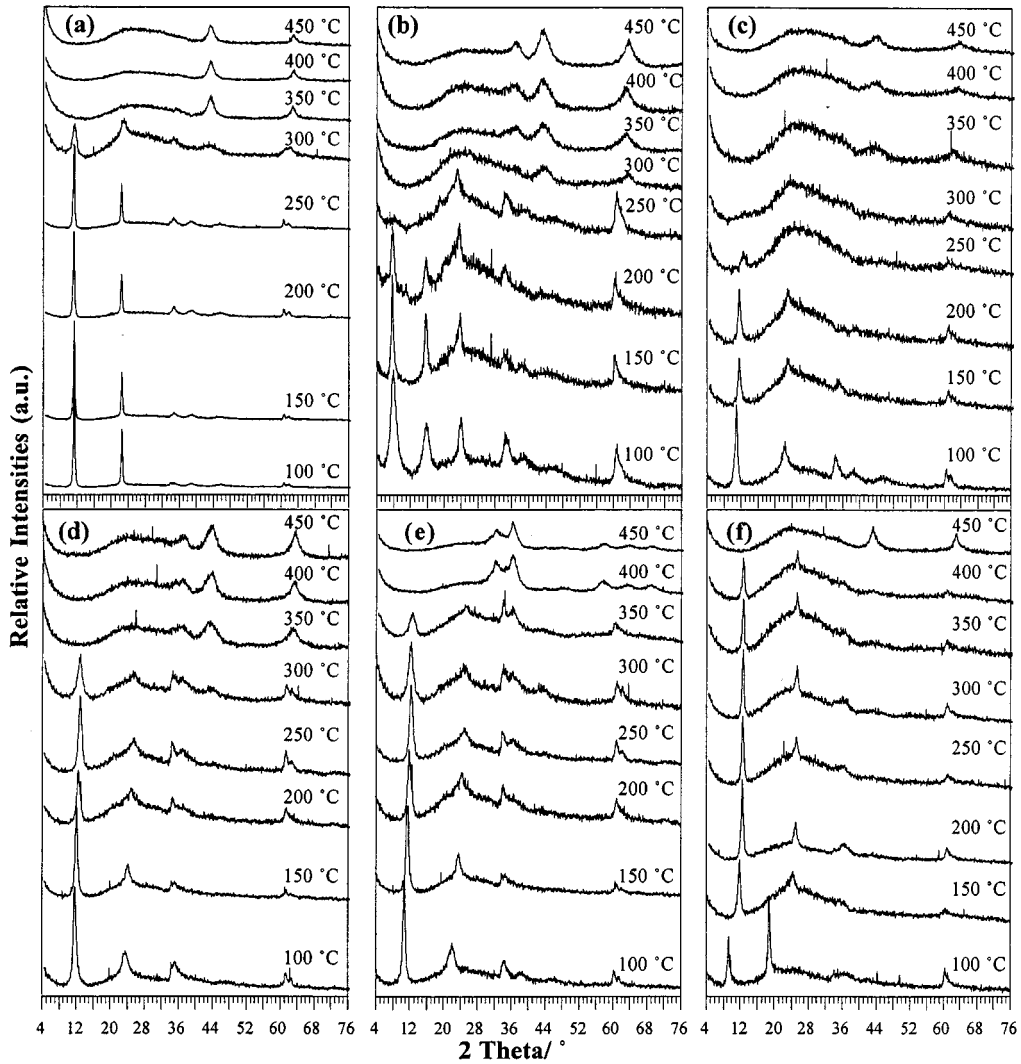

FIG. 3. XRPD patterns of (a) [Mg–Al–Cl], (b) [Mg–Al– $Fe(CN)_6$], (c) [Mg–Al–P_2O_7], (d) [Mg–Al–V_2O_7], (e) [Mg–Al– CrO_4], and (f) [Mg–Al–Cr_2O_7] hydrotalcites calcined at various temperatures.

structure. The anion would lose most of its original intrinsic characteristics (geometry, charge), which at the same time would inevitably result in the complete destruction of the lamellar structure and the formation of amorphous mixed oxides as evidenced by XRPD. With regard to the stability of the LDH phase as a function of the calcination temperature, the presence of the other oxo-anions proved to be quite beneficial. Here again the XRPD data are in good agreement with the thermal analyses: the maintenance of a hydrotalcite phase at relatively high temperature can most certainly be correlated with the delay in the dehydroxylation observed in the previous section.

A significant difference in the evolution of both the parent [Mg–Al–Cl] and [Mg–Al–$Fe(CN)_6$], when compared to the oxo-anion intercalated LDHs, is the absence of interlayer contraction with increasing temperature. For the oxo-anion intercalated LDHs the evolution of basal spacing as a function of calcination temperature is represented graphically in Fig. 4. Except for [Mg–Al–Cr_2O_7], all the other materials show a gradual shrinkage with increasing temperature until a limit value is achieved or the structure collapses. The dichromate anion proves thus to be the more disposed to undergo a grafting process with the host layers, exhibiting a contraction of 1.93 Å between 100 and 150°C. For this material we can note that, as with the thermogravimetric plateau observed between 200 and 300°C (Fig. 3), no further interlayer contraction occurs within a relatively wide range of temperature. It appears thus to confirm the enhanced stability of the LDH. The order of thermal stability, as determined by X-ray diffraction and thermogravimetric

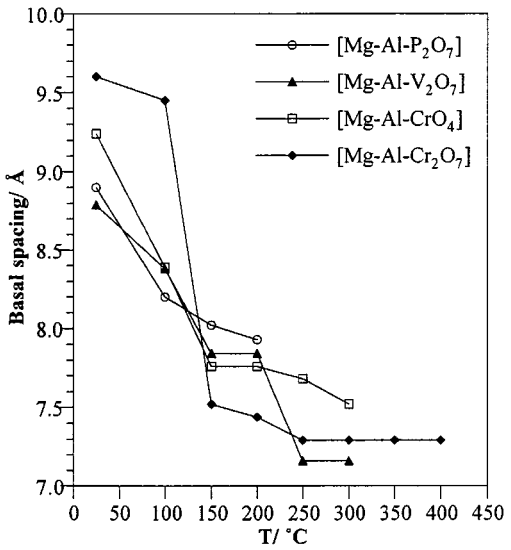

FIG. 4. Evolution of the interlamellar distance in Mg–Al hydrotalcites as a function of calcination temperature.

analyses for the LDHs investigated in this study would thus be

$$(Fe(CN)_6)^{3-} \approx (P_2O_7)^{4-} < (V_2O_7)^{4-} \approx Cl^- \ll (CrO_4)^{2-} < (Cr_2O_7)^{2-}.$$

The difference in the behavior of the $(X_2O_7)^{q-}$ anions would be most probably due to the relative stability of the anionic species and their reactivity toward the brucite-like sheets.

Case of the Chromate Oxo-anions

In order to better comprehend the guest–host interactions in the anion-exchanged hydrotalcites, a further detailed analysis of the chromate and dichromate LDHs is discussed hereafter. We first consider an infrared absorption spectroscopic study of the calcined phase: infrared analyses can provide us with useful information on the relative orientation of the anionic species within the interlamellar species. In Fig. 5 the possible symmetries for the chromate and dichromate species as imposed by the different types of interaction are schematized.

Figure 6 shows the spectra of [Mg–Al–CrO_4] and [Mg–Al–Cr_2O_7] calcined at different temperatures. We have reported here only those temperatures for which the X-ray diffraction patterns evidenced the existence of a lamellar structure. The evolution of the infrared spectra with increasing calcination temperature is very distinct depending on the anionic species under investigation.

The spectra of the chromate LDH clearly show the manifestation of an additional absorption band with increasing calcination temperature. In the untreated material only one band is assigned to the chromate species. However the apparition of a shoulder on the main absorption band after a mild thermal treatment at 100°C is compatible with a change in the symmetry of the anion. Upon calcination at higher temperatures, from 200°C up to 300°C, this shoulder develops into a clearly visible band centered at 928 cm^{-1}. This is most probably caused by a lowering in the symmetry of the (CrO_4) tetrahedra resulting in the splitting of the degenerate vibrations and activates the otherwise infrared inactive vibrations. There is also some modifications happening in the spectral window ranging from 650 through 800 cm^{-1}, but it is rather difficult to assign with absolute certainty these variations to the anionic entities due to possible overlapping with the lattice vibrations. On the other hand, assuming that these bands are to be assigned mainly to Mg–O and Al–O vibrations (33, 34), it then suggests that the brucite-like sheets are also affected by the reorganization of the interlayer. In which case, these observations further support the idea of a strong interaction of the anion with the hydroxylated sheets. Given that only one extra band is detected, it is more likely that the chromate anions interact with the LDH sheets through unidentate coordination. Bidentate coordination would imply further lowering of the symmetry and apparition of more bands.

As far as symmetry considerations are concerned, the dichromate intercalated LDHs behave in a way quite opposite to that of the chromate. Indeed, for [Mg–Al–Cr_2O_7] the disappearance of some absorption bands after moderate thermal treatment can be related to an increase in the symmetry of the anion. The fine band structures observed in the fresh material disappear completely after calcination at 100°C, which compared to the previous material indicates an important difference in the reactivity of the two anions. One possible reason for this might be related to the degree of solvation of the anion in the interlamellar domain. Both the chromate and the dichromate anions bear a -2 charge, which implies that their relative concentration will be

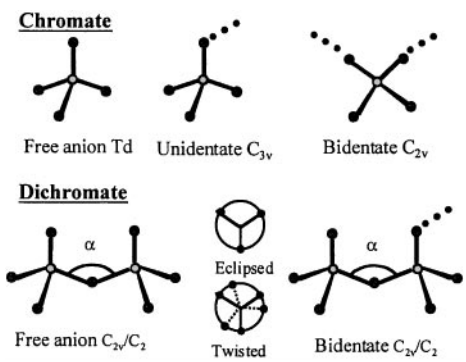

FIG. 5. Possible symmetries for the chromate and dichromate anions following grafting on the hydroxylated sheets.

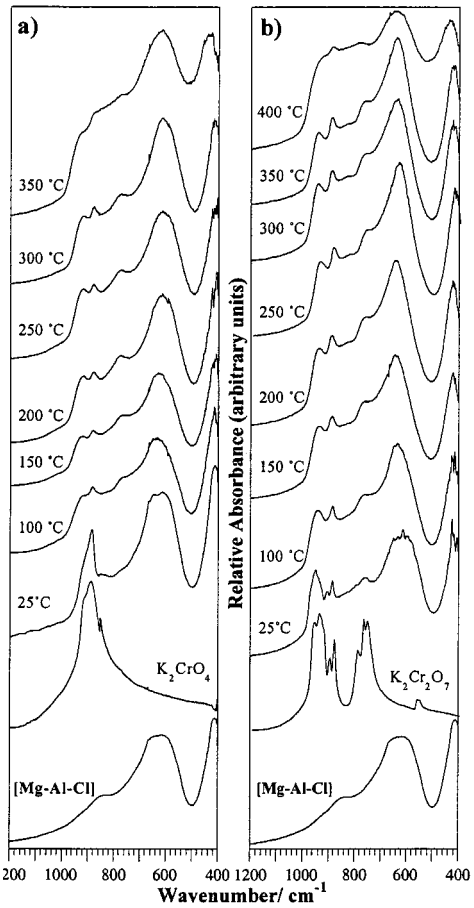

FIG. 6. Infrared spectra of (a) [Mg–Al–CrO_4] and (b) [MgAl–Cr_2O_7] calcined at different temperatures, compared to the chloride precursor and the respective potassium salt.

approximately the same. However, $(Cr_2O_7)^{2-}$ being twice as bulky as $(CrO_4)^{2-}$ will occupy more space, to the detriment of water molecules. This seems to be in good agreement with the XRPD data that reveal for this material a spontaneous shrinkage of the basal spacing at 150°C while for the chromate intercalated [Mg–Al] the change is more progressive, just like the evolution observed in the infrared spectra. The symmetry of the dichromate anion is probably C_2, with the terminal (CrO_3) groups being twisted rather than eclipsed. In either the free or the coordinated anion, any increase in symmetry can occur only through a rotation of these terminal groups to adopt an eclipsed conformation, giving a C_{2v} geometry. It can be pointed out that any small variation in the Cr–O–Cr angle will have no effect on the symmetry of the bidentate anion, the symmetry being imposed by the two terminal bonds. Unless the terminal oxygen are in the eclipsed position and the bond angle is stretched to 180°, in which case a C_2, normal to the Cr–O–Cr and passing through the bridging oxygen, is introduced in the molecule. It is also interesting to note that following calcination at 200°C and above, it becomes relatively difficult to distinguish between [Mg–Al–CrO_4] and [Mg–Al–Cr_2O_7]. The only difference lies in the position of the bands (928, 871, and 733 cm^{-1} in [Mg–Al–CrO_4] and 938, 882, and 748 cm^{-1} in [Mg–Al–Cr_2O_7]), which represent a slight shift (10 to 15 cm^{-1}) toward the higher frequencies for the dichromate-containing LDH. This would imply a stronger interaction with the brucite-like sheets and can explain the greater stability of the dichromate magnesium–aluminum. As with [Mg–Al–CrO_4] the same comment can be made here regarding the bands appearing in the region 650–850 cm^{-1}, which can be associated with minor modifications of the LDH framework.

These guest–host interactions, between the intercalated anion and the hydroxylated sheets, were further investigated by measuring their influence on the rehydration and anion-exchange properties of the dichromate magnesium–aluminum hydrotalcite. Rehydration of the heat-treated LDHs was carried out by reslurrying the material in deionized water, maintained under inert nitrogen atmosphere. The anion-exchange properties were assessed by performing a back exchange in a 0.25 M solution of sodium carbonate (25 cm^3 per gram of LDH). Carbonate anions are known to have the greatest affinity for hydrotalcite-like compounds. In all cases the reaction mixture was kept under vigorous magnetic stirring for 3 h. The X-ray powder diffraction patterns of the resulting phases are presented in Fig. 7.

When the material calcined at 100°C is rehydrated, a change in the basal spacing is observed: the LDH swells to almost the same interlayer distance as that of the fresh compound. As indicated in Fig. 4, the interlamellar contraction following calcination at 100°C is only 0.15 Å (d_{003} = 9.45 Å). This can be associated with the elimination of the crystallization water; the uptake of water on rehydration will thus contribute to the interlayer expansion. However, with the material calcined at 150°C no such expansion is observed. A similar trend occurs when carbonate anions are back-exchanged: the fresh dichromate LDH is fully exchanged, the diffraction pattern is shown to be characteristic of a carbonate phase. On the other hand, only a partial exchange is achieved when the temperature of the thermal treatment is increased to 100°C and the back-exchange is unsuccessful with [Mg–Al–Cr_2O_7] calcined at 150°C. This behavior is in good agreement with the previously reported data of Stanimirova *et al.* (35) on low temperature metaphases of magnesium–aluminum hydroxycarbonates. However an important difference was that their materials recovered the original interlayer spacing even after calcination at 260°C. The results presented here would thus suggest that the guest–host interactions involving the dichromate anion differ from those of the carbonate anion. The more likely explanation would be that the dichromate anion might interact on two hydroxylated sheets and tend to form permanent pillars. This would explain the failure of the

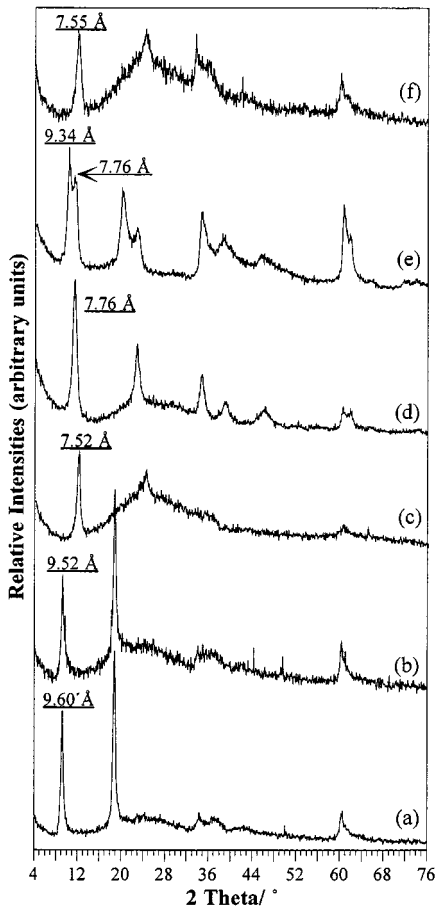

FIG. 7. XRPD patterns of [Mg–Al–Cr_2O_7]: (a) original, (b) calcined at 100°C and rehydrated, (c) calcined at 150°C and rehydrated, (d) back-exchanged with Na_2CO_3, (e) calcined at 100°C and back-exchanged, and (f) calcined at 150°C and back-exchanged.

rehydration and back-exchange in the materials calcined at 150°C. The calcination temperature appears to determine the extent of pillaring that can be achieved, as after a thermal treatment at 100°C some of anions are still exchangeable.

Surface Area of the Intercalated LDHs and Derived Mixed Oxides

To complete the study of these intercalated materials, their surface area and porosity properties have also been investigated, both for the fresh samples and samples calcined at 450°C. The main results are summarized in Table 3.

It is interesting to note how the specific surface area of the magnesium–aluminum hydrotalcite varies as the initial chloride anions are replaced by other anions. The high surface area of the hexacyanoferrate LDH has been ascribed by various authors (11, 23–25) to the presence of microporosity, which is here also confirmed with the highest micropore volume observed in the samples studied. Again this material exhibits a singular behavior when compared to the oxo-anion LDHs. The important point to consider is that the decrease in surface area observed after anion exchange is not solely due to the high charge density of the hydroxylated sheets. Some authors (23) have correlated the failure to induce microporosity in LDHs with this intrinsic property causing the anions to be "stuffed" in the interlayer rather than be intercalated. However, concerning the oxo-anions studied in this work, we would be more inclined to conclude that the inaccessibility of the interlamellar space is mostly due to the reactivity of the terminal oxygen groups. It is believed that the low surface area observed with the latter compounds is the result of guest–host interactions (grafting) following the heat treatment prior to the sorption measurement. This step is necessary to clean the surface of the solid from possible contaminant and mostly to remove adsorbed and interlayer water. It appears that, although a relatively low temperature of 80°C is used, the contraction of the interlamellar domain is enhanced by the use of reduced pressure during outgassing. The increase in surface area observed with the calcined chloride LDH, associated with a craterization process (19), does not seem to be reproducible with all the exchanged materials. The main reason would be that in these materials the anionic species are not volatile and would rather cause a compaction of the resulting mixed oxides. However, given the very different values obtained with the calcined LDHs, the more likely explanation is that the adsorptive capacity of the mixed oxides is affected by its chemical composition. This seems to be in agreement with the small change observed in the micropore volume of the calcined samples, while in some cases the surface area is considerably increased ([Mg–Al–Cr_2O_7] and [Mg–Al–V_2O_7]).

CONCLUSIONS

In this work, starting from a single-parent chloride hydrotalcite, subsequently exchanged with a variety of anions,

TABLE 3
Surface Area and Micropore Volume of As-Synthesized and Calcined Mg–Al LDHs

	Uncalcined		Calcined	
Interlamellar anion	Surface area ($m^2\,g^{-1}$)	Micropore volume ($cm^3\,g^{-1}$)	Surface area ($m^2\,g^{-1}$)	Micropore volume ($cm^3\,g^{-1}$)
Cl^-	45	0.018	191	0.075
$[Fe(CN)_6]^{3-}$	311	0.147	64	0.021
$(P_2O_7)^{4-}$	23	0.006	30	0.012
$(V_2O_7)^{4-}$	14	0.027	164	0.028
$(CrO_4)^{2-}$	13	0.019	24	0.011
$(Cr_2O_7)^{2-}$	42	0.026	110	0.024

we were in a better position to conduct a comparative investigation of their influence on the structural and thermal properties of the resulting LDHs. We have brought further evidence that the grafting process occurring between the intercalated anions and the hydroxylated sheets is the result of the reactivity of the terminal oxygen groups of oxoanions, as no such interaction was evidenced with the hexacyanoferrate species. A systematic study of the structural evolution under mild heat treatment has shown in some cases a very important shrinkage of the interlayer domain, which has also been related to a negative impact on the surface area. The thermogravimetric analyses have provided convincing evidence of the enhancement of the thermal stability of the magnesium–aluminum hydrotalcite through intercalation of chromate and dichromate anions. Nitrogen sorption experiments have shown that the interlayer accessibility is not only hindered by the presence of bulky anionic species but is also due to the interaction of the anions with the brucite-like sheets.

ACKNOWLEDGEMENT

F.M. acknowledges a grant from Université Blaise Pascal under a BRITE-EURAM project funded by the EC (Contract BREU-CT91-0480).

REFERENCES

1. M. C. Gastuche, C. Brown, and M. M. Mortland, *Clay Miner.* **7,** 177 (1967).
2. R. Allmann, *Chimica* **24,** 99 (1970).
3. S. Miyata, *Clays Clay Miner.* **23,** 369 (1975).
4. F. Cavani, F. Trifirò, and A. Vaccari, *Catal. Today* **11,** 173 (1991).
5. F. Trifirò and A. Vaccari, *in* "Comprehensive Supramolecular Chemistry" (J. L. Atwood, D. D. MacNicol, J. E. D. Davies, and F. Vögtle, Ed.), Vol. 7, Chap. 10, pp. 251–291, Pergamon, Oxford, 1996.
6. V. Rives and M. A. Ulibarri, *Coord. Chem. Rev.* **181,** 61 (1999).
7. O. Clause, M. Gazzano, F. Trifirò, A. Vaccari, and L. Zatorski, *Appl. Catal.* **73,** 217 (1995).
8. F. Malherbe, C. Forano, B. Sharma, M. P. Atkins, and J. P. Besse, *Appl. Clay Sci.* **13,** 381 (1998).
9. F. Malherbe, C. Depege, C. Forano, M. P. Atkins, B. Sharma, S. R. Wade, and J. P. Besse, *Appl. Clay Sci.* **13,** 451 (1998).
10. S. Miyata, *Clays Clay Miner.* **11,** 305 (1983).
11. F. A. P. Cavalcanti, A. Schultz, and P. Biloen, "Preparation of Catalysts IV" (B. Delmon, P. Grange, P. A. Jacobs, and G. Poncelet, Eds.), pp. 165–174, Elsevier, Amsterdam, 1987.
12. J. Twu and P. Dutta, *J. Phys. Chem.* **93,** 7863 (1989).
13. S. Miyata and A. Okida, *Clays Miner.* **25,** 14 (1977).
14. A. de Roy, C. Forano, K. El Malki, and J. P. Besse, *in* "Synthesis of Microporous Materials" (M. L. Occelli and H. E. Robson, Eds.), pp. 108–169, Van Nostrand–Reinhold, New York, 1992.
15. E. P. Barrett, L. G. Joyner, and P. H. Halenda, *J. Am. Chem. Soc.* **73,** 373 (1951).
16. M. Pourbaix, "Atlas d'équilibres électrochimiques," Gauthier–Villars, Paris, 1963.
17. K. S. Han, L. Guerlou-Demourgues, and C. Delmas, *Solid State Ionics* **84,** 227 (1996).
18. M. Ménétrier, K. S. Han, L. Guerlou-Demourgues, and C. Delmas, *Inorg. Chem.* **36,** 2441 (1997).
19. W. T. Reichle, S. Y. Kang, and D. S. Everhardt, *J. Catal.* **101,** 352 (1986).
20. G. Mascolo and O. Marino, *Miner. Mag.* **43,** 619 (1980).
21. O. Marino and G. Mascolo, *Thermochim. Acta.* **55,** 377 (1982).
22. D. R. Lide (Ed.), "The Handbook of Chemistry and Physics," 17th ed., CRC Press, Boca Raton, FL, 1997.
23. H. Nijs, M. De Bock, and E. F. Vansant, *Microp. Mesop. Mater.* **30,** 243 (1999).
24. A. Berés, I. Palinko, I. Kiricsi, J. B. Nagy, Y. Kiyozumi, and F. Mizukami, *Appl. Catal. A* **182,** 237 (1999).
25. M. J. Holgado, V. Rives, M. S. Sanroman, and P. Malet, *Solid State Ionics* **92,** 273 (1996).
26. F. Malherbe, L. Bigey, C. Forano, A. de Roy, and J. P. Besse, *J. Chem. Soc. Dalton Trans.* **21,** 3831 (1999).
27. K. El Malki, A. de Roy, and J. P. Besse, *Eur. J. Solid State Inorg. Chem.* **26,** 339 (1989).
28. C. Depège, C. Forano, A. de Roy, and J. P. Besse, *Mol. Cryst. Liq. Cryst.* **244,** 161 (1994).
29. V. R. L. Constantino and T. J. Pinnavaia, *Inorg. Chem.* **34,** 883 (1995).
30. C. Depege, L. Bigey, C. Forano, A. de Roy, and J. P. Besse, *J. Solid State Chem.* **126,** 314 (1996).
31. M. del Arco, V. Rives, R. Trujillano, and P. Malet, *J. Mater. Chem.* **6,** 1419 (1996).
32. L. Bigey, C. Depège, A. de Roy, and J. P. Besse, *J. Phys. IV (C2)* **7,** 949 (1997).
33. C. J. Serna, J. L. White, and S. L. Hern, *Clays Clay Miner.* **25,** 384 (1977).
34. M. J. H. Hernandez-Moreno, M. A. Ulibarri, J. L. Rendon, and C. J. Serna, *Phys. Chem. Miner.* **12,** 34 (1985).
35. T. S. Stanimirova, I. Vergilov, G. Kirov, and N. Petrovna, *J. Mater. Sci.* **34,** 3153 (1999).